Simulation of platelet adhesion and aggregation regulated by fibrinogen and von Willebrand factor

Daisuke Mori[1], Koichiro Yano[2], Ken-ichi Tsubota[3], Takuji Ishikawa[1], Shigeo Wada[4], Takami Yamaguchi[1]

[1]Deptartment of Bioengineering and Robotics, Tohoku University, Japan; [2]Toyota Motor Corporation, Japan; [3]Department of Electronics and Mechanical Engineering, Chiba University, Japan; [4]Department of Mechanical Science and Bioengineering, Osaka University, Japan

Summary

We propose a method to analyze platelet adhesion and aggregation computationally, taking into account the distinct properties of two plasma proteins, von Willebrand factor (vWF) and fibrinogen (Fbg). In this method, the hydrodynamic interactions between platelet particles under simple shear flow were simulated using Stokesian dynamics based on the additivity of velocities. The binding force between particles mediated by vWF and Fbg was modeled using the Voigt model. Two Voigt models with different properties were introduced to consider the distinct behaviors of vWF and Fbg. Our results qualitatively agreed with the general observation of a previous in-vitro experiment, thus demonstrating that the significant development of thrombus formation in height requires not only vWF, but also Fbg. This agreement of simulation and experimental results qualitatively validates our model and suggests that consideration of the distinct roles of vWF and Fbg is essential to investigate the physiological and pathophysiological mechanisms of thrombus formation using a computational approach.

Keywords

Computational simulation, glycoprotein receptors, thrombus, shear flow

Thromb Haemost 2008; 99: 108–115

Introduction

The formation of a thrombus is a critical phenomenon both physiologically and pathologically. Physiologically, it plays an important role in haemostatic function. In a diseased state such as arteriosclerosis, however, thrombus formation can be the cause of a fatal disease process, e.g. myocardial infarction, which blocks the blood supply to the periphery of the body (1). In contrast, the failure of thrombus formation because of platelet dysfunction, as in Glanzmann thrombasthenia and von Willebrand disease (vWD), produces a critical bleeding tendency (2). A better understanding of the mechanism of thrombus formation could help to elucidate the physiological haemostatic mechanisms and the pathology of thrombosis and bleeding disorders, which will ultimately contribute to improvements in the treatment of these diseases through antiplatelet drugs and the development of artificial platelets.

Although thrombus formation is regulated through a series of physiological and biochemical processes, various mechanical factors are involved. First, a thrombus is formed under the fluid mechanical conditions of blood flow. Platelet adhesion and aggregation are highly dependent on the magnitude of the shear rate induced by blood flow (3–5). Additionally, platelet adhesion and aggregation occur through a process in which protein molecules present in the blood plasma bind to glycoprotein (GP) receptors on the surface of platelets to form intercellular molecular bridges (1, 6–12). Thus, a thrombus can be regarded as a mechanical structure constructed by the platelets through physical interaction with plasma protein molecules.

Numerous computational simulations have been used to investigate the complexity of blood coagulation. Various methods have been proposed to simulate platelet adhesion and aggregation under blood flow from a mechanical point of view, with platelet-platelet or platelet-surface interactions mediated by biomolecular bridges that have been incorporated into established computational fluid dynamics models (13–17). In addition, the formation and destruction of a primary thrombus under blood flow has been analyzed computationally using the discrete element method in which the model is based on the physiological nature of the platelets as discrete objects (18, 19). These computational simulations have qualitatively demonstrated the growth and collapse of a thrombus caused by blood flow and intercellular molecular bridges and verified the importance of these bridges in thrombus formation.

Although these types of computational simulations are powerful tools for clarifying the mechanisms of thrombus

Correspondence to:
Daisuke Mori
Department of Bioengineering and Robotics
Tohoku University
6–6–01 Aoba, Aoba-ku, Sendai, Miyagi 980–8579, Japan
Tel.: +81 22 795 6958, Fax: +81 22 795 6958
E-mail: daisuke@pfsl.mech.tohoku.ac.jp

Received August 3, 2007
Accepted after minor revision October 18, 2007

Prepublished online December 5, 2007
doi:10.1160/TH07–08–0490

formation that involve biomolecular interactions that occur under blood flow, models of intercellular molecular bridges have been too simple. These molecular bridges have been formulated with only a single linkage (13–19), even though various types of plasma proteins with distinct roles are involved in platelet adhesion and aggregation. Of the plasma proteins, von Willebrand factor (vWF) and fibrinogen (Fbg) are thought to be major participants in platelet adhesion and aggregation because of bleeding disorders that are associated with their deficiencies (20–22). For example, subjects with vWD are deficient in vWF, but have normal levels of other plasma proteins. Fbg and vWF, which promote adhesion and aggregation by binding preferentially to the platelet membrane receptors GP IIb/IIIa and GP Ibα, have highly distinct properties. For example, Savage et al. (4) investigated platelet interaction with Fbg or vWF immobilized on a glass cover slip placed in a parallel plate flow chamber under various wall shear rates to determine the properties of Fbg and vWF. They found that Fbg preferentially binds with GP IIb/IIIa, and the binding is irreversible and efficient at relatively low shear rates (i.e. 50–500 s^{-1}). In contrast, vWF binds exclusively with GP Ibα and binds somewhat with GP IIb/IIIa, and the GP Ibα-dependent binding is reversible or transient and more efficient at relatively high shear rates than at low rates (4). These distinctive properties of Fbg and vWF should be taken into account in computational simulations. These differences may be significant in attempting to better understand the mechanisms of bleeding disorders and assess pharmacological treatments for thrombosis. Current pharmacological treatment for thrombosis involves an inhibitor that blocks a specific glycoprotein receptor; thus, it does not necessarily affect both vWF- and Fbg-dependent binding.

Thus, we investigated the effects of the distinct properties of vWF and Fbg on the process of platelet adhesion and aggregation on an injured surface using a computational simulation. We used a general framework that was developed to examine the collapse process of a primary thrombus using Stokesian dynamics based on the additivity of velocities (18, 19). However, we modified the model of the intercellular molecular linkage to address the distinct properties of Fbg and vWF, including their receptors GP IIb/IIIa and GP Ibα. We conducted computations for four different situations: no receptor deficiency, deficiency of GP IIb/IIIa, deficiency of GP Ibα, and deficiency of both GP IIb/IIIa and GP Ibα. We compared our simulation results with previously published in-vitro experimental results in which the efficiency of platelet adhesion and aggregation under fluid shear were investigated using plasma anti-receptor inhibitors (5).

Methods

The general framework that we used follows Stokesian dynamics based on the approximation of the additivity of velocities, which was used by Satoh et al. (23, 24) to examine ferromagnetic colloidal dispersions. We recently modified the method and developed an in-house numerical code to simulate the collapse process of a primary platelet thrombus by modeling the binding force mediated by the plasma proteins in place of magnetic force (19). Here, we improved the model to deal with the binding force caused by two distinct plasma proteins, i.e. Fbg and vWF.

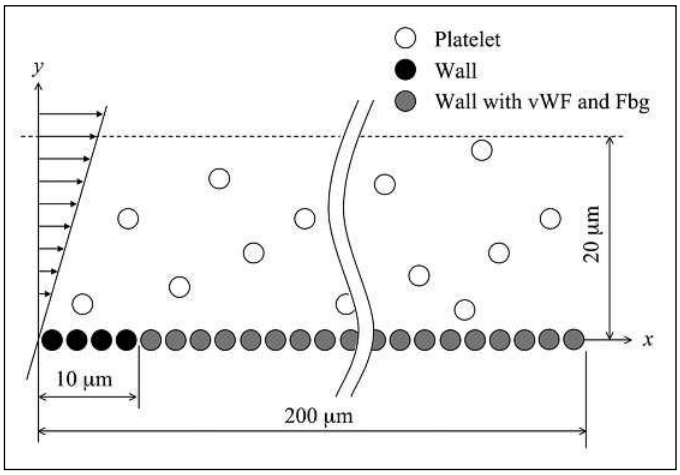

Figure 1: Schematic illustration of the monolayer model for the motion of platelets near the blood vessel wall under simple shear flow. Platelets were idealized as solid spherical particles 2 μm in diameter. The platelet particles were randomly positioned in the initial configuration and inserted at the upstream end on x = 0 μm within y = 0–20 μm. The blood vessel wall was modeled as a large number of solid spheres with diameter identical to that of the platelets. It was assumed that the blood vessel wall particles downstream from x = 10 μm possess vWF and Fbg plasma proteins. A simple shear flow with a shear rate of 5,000 s^{-1} was imposed as the background flow.

Stokesian dynamics

Stokesian dynamics is a powerful method by which to trace the motions of multiple particles in a suspension; it accurately accounts for the hydrodynamic interactions between particles. Although the approximation of the additivity of velocities is inferior to the approximation of the additivity of forces (25) in the reproduction of the lubrication effect, the calculation of the inverse matrix is unnecessary in the simulations (23, 24). Thus, the additivity of velocities can considerably reduce the computational time, which means that it is applicable to larger systems. Because we are interested in thrombus formation, which involves a large number of platelets, a large system is desirable. Moreover, the lubrication effect is thought to be insignificant in this system because binding forces are dominant when the platelets are close to each other.

We computed the motions of platelets near the blood vessel wall boundary, where a simple shear background flow is imposed (Fig. 1). The blood vessel wall is modeled as a large number of solid spheres. The platelets are also idealized as solid spheres with the same radius as those in the blood vessel wall. Although this idealization is a major simplification, activated platelets have more of a spherical shape than a disc shape (26). Activated platelets possess extensive pseudopodia, but there is no accepted model that appropriately deals with objects with similar complex shapes. The plasma, which is the dispersed medium in our system, was assumed to be an incompressible Newtonian fluid. Because the size of a platelet is about 2 μm, we can assume that the flow field around platelets is governed by the Stokes equation.

Stokesian dynamics based on the additivity of velocities caused by the force exerted on a particle yields a particle velocity of:

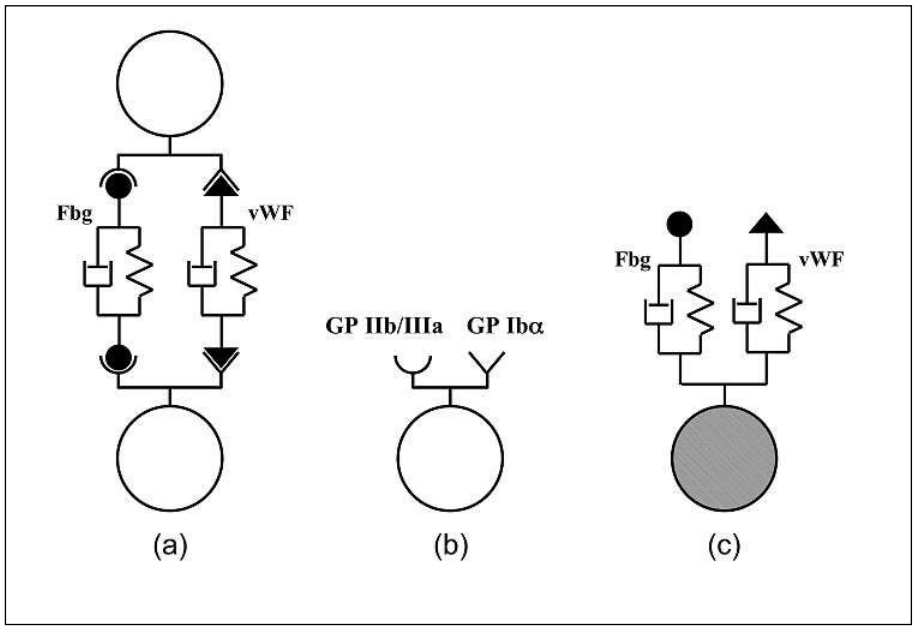

Figure 2: Model for platelet-platelet aggregation and platelet-surface adhesion via plasma proteins and glycoproteins (GPs). The force induced between two platelet particles through two plasma proteins, i.e. vWF and Fbg, were modeled using a Voigt model, which was composed of a parallel spring and dashpot (a). Two Voigt models with different parameters were used to express the proteins' distinct properties. GP IIb/IIIa and GP Ibα, which are the main receptors for Fbg and vWF, respectively, were modeled on the platelet particle to reproduce the selective association of the plasma proteins with the receptors (b). Similarly, the force induced between the platelet particles and blood vessel wall with vWF and Fbg was modeled (c).

$$\boldsymbol{v}_\alpha = \boldsymbol{U}(\boldsymbol{r}_\alpha) + \frac{1}{\eta}\left\{\frac{1}{6\pi a}\boldsymbol{F}_\alpha + \sum_{\beta=1(\neq\alpha)}^{N}\left(\boldsymbol{a}_{\alpha\alpha} - \frac{1}{6\pi a}\boldsymbol{I}\right)\cdot\boldsymbol{F}_\alpha + \sum_{\beta=1(\neq\alpha)}^{N}\boldsymbol{a}_{\alpha\beta}\cdot\boldsymbol{F}_\beta\right\} + \sum_{\beta=1(\neq\alpha)}^{N}\tilde{\boldsymbol{g}}_\alpha : \boldsymbol{E} \quad (1)$$

where $\boldsymbol{U}(\boldsymbol{r}_\alpha)$ is the velocity of the background flow field at the position of particle α. $\boldsymbol{F}_i$ (i = α, β) is the force acting on particle i; a is the particle radius, $\boldsymbol{E}$ is the background rate-of-strain tensor; $\boldsymbol{I}$ is the unit tensor; $\boldsymbol{a}_{ij}$ and $\tilde{g}_i$ are the mobility tensors; and N is the number of particles in the system (23, 24). The mobility tensors $\boldsymbol{a}_{ij}$ and $\tilde{g}_i$ relate particle velocities to forces acting on each particle, and rate-of-strain of the background flow, respectively. Values for the mobility tensors can be found in standard texts, e.g. Kim and Karrila (27). We considered

$$\boldsymbol{F}_i = \boldsymbol{F}_i^{(b)} + \boldsymbol{F}_i^{(c)} \quad (2)$$

where $\boldsymbol{F}_i^{(b)}$ is the binding force induced between particles by the plasma proteins and $\boldsymbol{F}_i^{(c)}$ is the contact force induced by the collision of particles. The fluid flow and adhesion processes are coupled by substituting equation 2 into equation 1. Through this process, the velocity of a particle can be obtained under multibody hydrodynamic interactions along with the forces acting on each particle from equation 1.

Since the platelets are too large for Brownian motion to become important, it does not appear in equation 1. We ignored the difference in density between the plasma and the platelets. The rotational motion of particles was also ignored because the rotational velocity at $\boldsymbol{r}$ due to the torque exerted on a particle at the origin of the coordinate system decays as r^{-2}, where r is the distance, in the far field. In contrast, the velocity at $\boldsymbol{r}$ due to the force exerted on a particle at the origin of the coordinate system decays as r^{-1}, which is much larger in the far field (27). The particle positions were updated using Euler's method:

$$[\boldsymbol{r}_\alpha]_{t+\Delta t} = [\boldsymbol{r}_\alpha]_t + \Delta t[\boldsymbol{v}_\alpha]_t \quad (3)$$

where the subscripts t and $t + \Delta t$ indicate the current and next time step, respectively.

Modeling the binding force mediated by plasma proteins

We assumed that the binding force, $\boldsymbol{F}_i^{(b)}$, is induced exclusively by two plasma proteins, i.e. Fbg and vWF, which are the main participants in platelet adhesion and aggregation. These proteins have highly distinct properties. To express this distinction, we prepared two Voigt models, each of which possessed different parameters (Fig. 2a). The spring reproduces a chemical energy change induced by the extension of macromolecules, and the dashpot the flow resistance occurred in stretching the coiled macromolecules. The preferential combination with GP Ibα or GP IIb/IIIa was modeled by considering receptors on the platelet particles (Fig. 2b). The associations between two specific particles due to the Fbg and vWF models were assumed following experimental observations (4) as follows: the association mediated by the Fbg model was formed when GP IIb/IIIa receptors occurred on both particles; the association mediated by the vWF model was formed when GP Ibα receptors occurred on both particles.

Fbg and vWF occur as long-chain macromolecules in the plasma. For example, vWF forms a multimer that can have molecular weights of 500,000–2,000,000 *M*. The structure is filamentous with a diameter of 2–3 nm and a length of up to 1,300 nm, approaching the diameter of a platelet, or loosely coiled with an apparent diameter of 200–300 nm (7). The size is functionally well regulated because of factors of fluid mechanics such as shear stress. To reproduce their function as long-chain protein molecules, we assumed that a binding force between two particles i and j can be formed when the particles become close to each other within a specific distance of $L_0 = 0.5$ μm, i.e. $|\boldsymbol{s}| \leq L_0$ is satisfied, where $\boldsymbol{s}$ indicates the separation vector expressed as

$$\boldsymbol{s} = \frac{\boldsymbol{r}_j - \boldsymbol{r}_i}{|\boldsymbol{r}_j - \boldsymbol{r}_i|}\{|\boldsymbol{r}_j - \boldsymbol{r}_i| - 2a. \quad (4)$$

In addition to these qualifications, we set the following distinctive rules for Fbg-GP IIb/IIIa and vWF-GP Ibα associations.

To reproduce the efficiency of the Fbg-GP IIb/IIIa association at low shear rates (4), we assumed that the Fbg-GP IIb/IIIa association is formed only when the difference in velocity between two particles is less than a specific value, $U_{act} = 5.5 \times 10^{-2}$ [m/s]: $|\boldsymbol{v}_j - \boldsymbol{v}_i| \leq U_{act}$. In contrast, to reproduce the reversibility of vWF-GP Ibα associations (4), we assumed that the vWF-GP Ibα association persists only for a specific time, $T_{act} = 0.5$ [s]. Additionally, we assumed that the dissociation occurs when $|\boldsymbol{s}|$ exceeds εL_0: $|\boldsymbol{s}| > \varepsilon L_0$, where ε is the maximum stretch of the spring and is 1.05. Note that, for the vWF-GP Ibα association, such threshold of difference in velocity as U_{act} in Fbg-GP IIb/IIIa association was not assigned. These rules are qualitatively consistent with former experimental observations (4).

The Voigt models were set to resist only against the stretch, and the force exerted between the particles *i* and *j* is given by

$$\boldsymbol{F}_{ij}^{(p)} = \frac{\boldsymbol{s}}{|\boldsymbol{s}|}\left[K^{(p)}\{|\boldsymbol{s}| - L_0\} - \eta^{(p)}\frac{|\Delta \boldsymbol{s}|}{\Delta t}\right] \quad (5)$$

where $K^{(p)}$ and $\eta^{(p)}$ are the spring elastic modulus and the damper viscous coefficient, respectively, and Δt is a time interval. The force expressed by equation 5 was calculated for each Voigt model. The parenthetic superscript (*p*) is replaced with (*vWF*) or (*Fbg*). Eventually, the binding force acting on a particle *i* is expressed as

$$\boldsymbol{F}_i^{(b)} = \sum_j \boldsymbol{F}_{ij}^{(vWF)} + \sum_j \boldsymbol{F}_{ij}^{(Fbg)}. \quad (6)$$

Contact force

Essentially, the lubrication effect caused between nearly touching particles induces a very large hydrodynamic force that deters the direct collision of the particles. Stokesian dynamics has the ability to reproduce the lubrication effect. In our system, however, introducing the binding force caused by the plasma proteins and the approximation of the additivity of forces induces the collision of particles. As in a previous study (18), we modeled the contact force caused by the collision using the Voigt model, similar to the binding force, but the contact force was assumed to occur only when the particles satisfied:

$$|\boldsymbol{r}_j - \boldsymbol{r}_i| - 2a \leq 0. \quad (7)$$

The force is expressed as:

$$\boldsymbol{F}_{ij}^{(c)} = \frac{\boldsymbol{s}}{|\boldsymbol{s}|}\left[K^{(c)}|\boldsymbol{s}| - \eta^{(c)}\frac{|\Delta \boldsymbol{s}|}{\Delta t}\right], \quad (8)$$

where $K^{(c)}$ and $\eta^{(c)}$ are the spring elastic modulus and the damper viscous coefficient, respectively. Here, the spring expresses the elastic collision, and the dashpot the resistance induced by the surrounding fluid. The contact force acting on a particle *i* is expressed as

$$\boldsymbol{F}_i^{(c)} = \sum_j \boldsymbol{F}_{ij}^{(c)}. \quad (9)$$

Conditions for the simulation

We considered a monolayer system in which the centers of particles are in the same *x*-*y* plane, although the flow field is fully three-dimensional (Fig. 1). The monolayer is used to reduce the computational load; we could thus simulate a blood vessel wall boundary of 200 μm in length. A simple shear flow in the *x*-*y* plane with a shear rate of $\dot{\gamma} = 5{,}000\ s^{-1}$ was imposed as the background flow field, which is expressed as $\boldsymbol{U}(\boldsymbol{r}) = \dot{\gamma} y \delta_x$. For this case, the rate-of-strain tensor $\boldsymbol{E}$ has only E_{xy} and E_{yx} as non-zero components such that $E_{xy} = E_{yx} = \dot{\gamma}/2$. The viscosity of the dispersed medium was assumed to be that of water, i.e. $\mu = 0.797 \times 10^{-3}$ Pa s. The blood vessel wall surface was modeled as discrete spherical particles of 2.0 μm in diameter that were lined on $y = 0$. The motion of the blood vessel wall particles was constrained. Platelet particles were continuously inserted at random vertical positions within $y = 1$–20 μm on $x = 0$ μm. Because few properties of the plasma proteins are known, we conducted supplemental simulations with $K^{(vWF)} = 6.0 \times 10^8$ N/m, $\eta^{(vWF)} = 3.3 \times 10^{-3}$ N/(m/s), $K^{(Fbg)} = 1.2 \times 10^9$ N/m, and $\eta^{(Fbg)} = 4.6 \times 10^{-3}$ N/(m/s). We have found that these parameter settings are critical, with which the stability of thrombus formation starts to break. We consider that it is important to understand the mechanical phenomenon at this critical point. Similarly, for the properties of the Voigt model for the contact force, we set $K^{(c)} = 4.0 \times 10^5$ N/m and $\eta^{(c)} = 8.4 \times 10^{-5}$ N/(m/s), obtained from supplemental simulations. These parameter values affected the results quantitatively, but not qualitatively. However, the results obtained using these parameters agreed well with previous experimental results (5). The time increment Δt was set at 1.0×10^{-9} s. The parameter settings are summarized in Table 1.

We analyzed four different cases in which the GP Ibα or GPIIb/IIIa receptors were selectively blocked. These cases mimicked the conditions of previous in-vitro experiments (5) in which platelet adhesion and aggregation were estimated under the selective inhibition of GP Ibα or GP IIb/IIIa. In case 1, both of the receptors were inhibited; in case 2, only GP IIb/IIIa was in-

Table 1: Parameters used for the background flow field, the disperse medium, the particle, the contact force model, and the Voigt model for vWF and Fbg.

Background flow field	Shear rate	$\dot{\gamma} = 5000\ [s^{-1}]$
Disperse medium	Viscosity	$\mu = 0.797 \times 10^{-3}$ [Pa.s]
Particle	Radius	$a = 1.0$ [μm]
Contact force model	Elastic modulus	$K^{(c)} = 4.0 \times 10^5$ [N/m]
	Viscous coefficient	$\eta^{(c)} = 8.4 \times 10^{-5}$ [N/(m/s)]
Voigt model for vWF	Elastic modulus	$K^{(vWF)} = 6.0 \times 10^8$ [N/m]
	Viscous coefficient	$\eta^{(vWF)} = 3.3 \times 10^{-3}$ [N/(m/s)]
	Natural length	$L_0 = 0.5$ [μm]
	Maximum stretch	$\varepsilon = 1.05$
	Duration	$T_{act} = 0.5$ [s]
Voigt model for Fbg	Elastic modulus	$K^{(Fbg)} = 1.2 \times 10^9$ [N/m]
	Viscous coefficient	$\eta^{(Fbg)} = 4.6 \times 10^{-3}$ [N/(m/s)]
	Natural length	$L_0 = 0.5$ [μm]
	Maximum stretch	$\varepsilon = 1.05$
	Threshold	$U_{act} = 5.5 \times 10^{-2}$ [m/s]

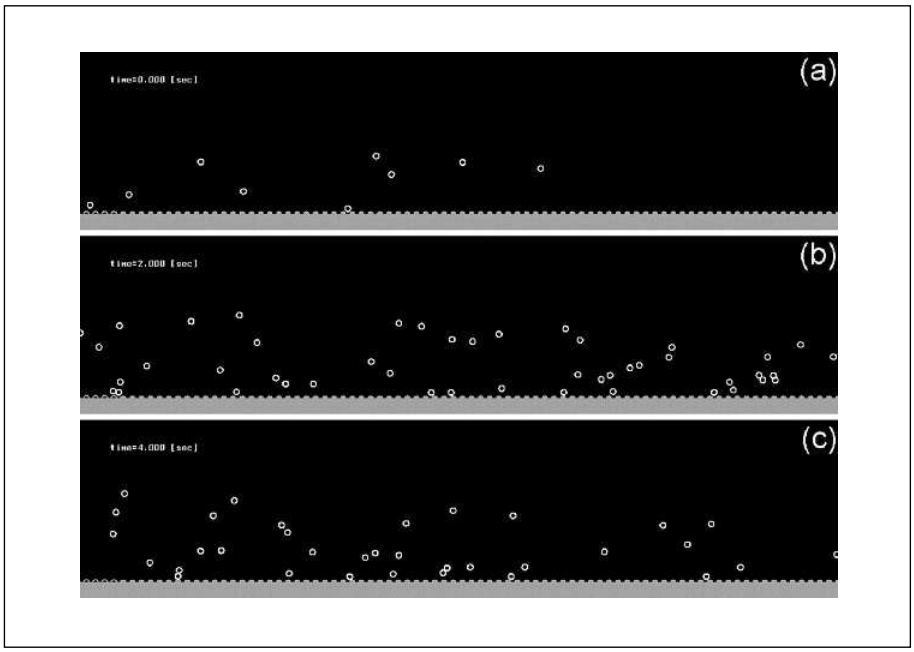

Figure 3: Configurations of platelet particles at three different time points in the computation for case 1, in which both receptors were inhibited. a) t = 0.0 s. b) t = 2.0 s. c) t = 4.0 s. Neither platelet adhesion nor platelet aggregation occurred because of the fully inhibited receptors.

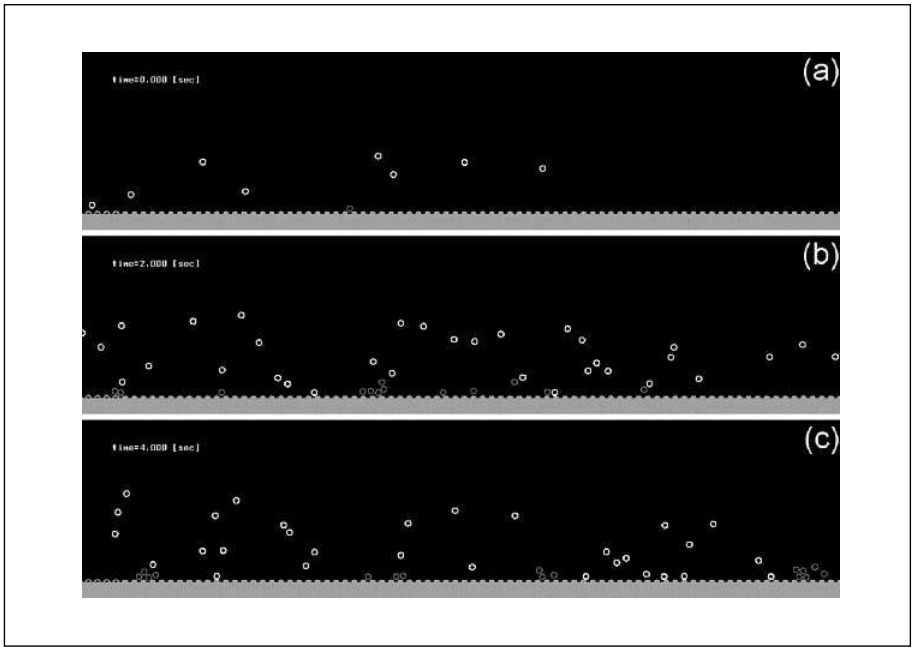

Figure 4: Configurations of platelet particles at three different time points in the computation for case 2, in which only GP IIb/IIIa receptors were inhibited. a) t = 0.0 s. b) t = 2.0 s. c) t = 4.0 s. Particles flowing near the blood vessel wall could transiently adhere onto the wall via the vWF-GP Ibα interaction, indicated by gray open circles. This transient adhesion did not lead to stable aggregation.

hibited; in case 3, only GP Ibα was inhibited; and in case 4, neither of the receptors were inhibited. We assumed that the blood vessel wall particles possessed the Voigt models for both vWF and Fbg, reproducing the blood vessel walls on which vWF and Fbg are immobilized (Fig. 2c). In all four cases, the initial configuration of the particles and the position and time at which the particles were inserted were identical.

Results and discussion

In case 1, in which both receptors were inhibited, neither platelet adhesion nor platelet aggregation occurred (Fig. 3). In case 2, in which only GP IIb/IIIa receptors were inhibited, the particles flowing near the blood vessel wall adhered onto the wall via the vWF-GP Ibα interaction (Fig. 4). However, the particles did not irreversibly adhere to the wall because the vWF–GP Ibα interaction is transient. Thus, a platelet aggregate did not form on the wall, although slight incidental platelet aggregation occurred. In cases 3 and 4, in which the GP IIb/IIIa receptors were functional, an irreversible platelet adhesion occurred because of the Fbg-GP IIb/IIIa interaction (Figs. 5 and 6). In these two cases, the adhered platelets subsequently recruited additional flowing platelets, leading to platelet aggregation that built up a thrombus in a vertical direction from the blood vessel wall. In case 4, the as-

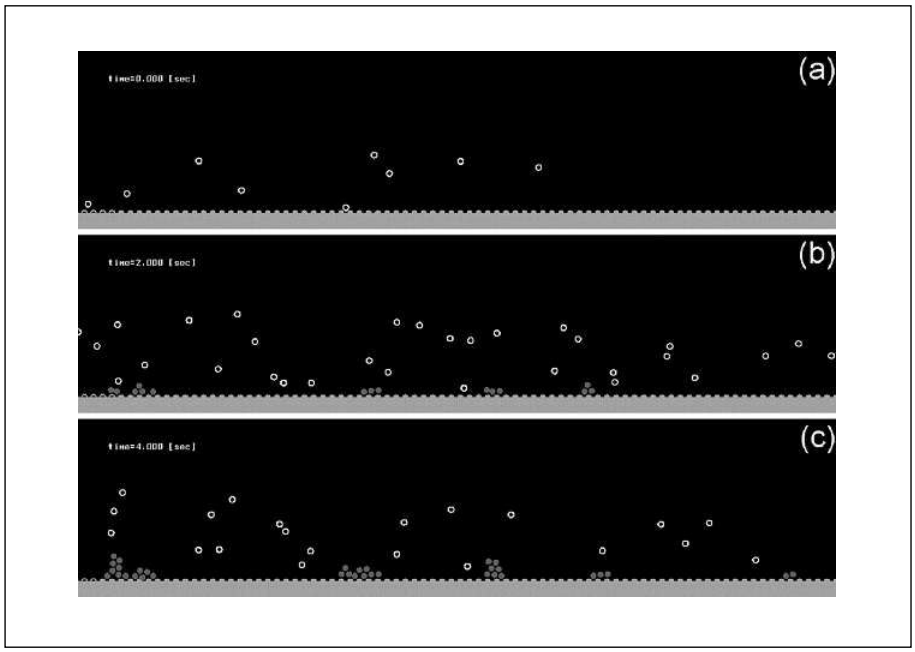

Figure 5: Configurations of platelet particles at three different time points in the computation for case 3, in which only GP Ibα receptors were inhibited. a) t = 0.0 s. b) t = 2.0 s. c) t = 4.0 s. Platelet adhesion occurred irreversibly because of the Fbg-GP IIb/IIIa interaction, indicated by gray filled circles. The adhered platelets recruited additional flowing platelets, leading to platelet aggregation. The formed aggregates reached up to 10 μm in height, but did not develop higher because the difference in velocity between the flowing platelets and those at rest on the aggregate exceeded the threshold, defined as U_{act}.

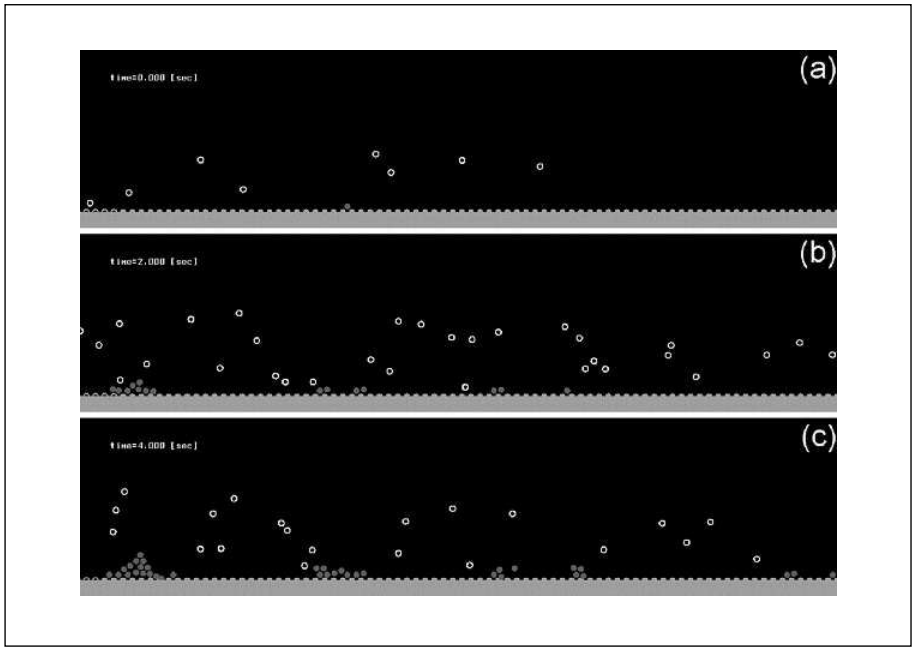

Figure 6: Configurations of platelet particles at three different time points in the computation for case 4, in which there was no receptor inhibition. a) t = 0.0 s. b) t = 2.0 s. c) t = 4.0 s. In contrast to case 3, the aggregate developed higher than 10 μm. Even at high positions where there was a great difference in velocity between flowing and aggregated particles, flowing particles could join the aggregation via the vWF-GP Ibα interaction. This aggregation caused by the vWF-GP Ibα interaction allowed the particles to aggregate firmly through the Fbg-GP IIb/IIIa interaction, leading to more significant development of the aggregate than in case 3.

sociation and the dissociation of vWF-GP Ibα interaction are repeated between the platelets forming the thrombus on the wall, although the thrombus is maintained because of the co-existence of the Fbg-GP IIb/IIIa interaction.

To estimate the extent of adhesion and aggregation, we measured the number of platelet particles that adhered to the blood vessel wall (Fig. 7) and the maximum height of the aggregates (Fig. 8). A significant increase in the number of adhered platelets over time occurred only in cases 3 and 4. The difference between these two cases in the number of adhered platelets was not remarkable, although the number tended to be somewhat larger in case 4 than in case 3 and approached 45 and 50 at 30 s in cases 3 and 4, respectively (Fig. 7). Eventually, platelets covered almost the entire surface of the blood vessel wall (results not shown). In contrast, in case 2, the number of adhered platelets remained at less than 20.

The thrombus height did not develop higher than about 12 μm in case 3 (Fig. 8) because the difference in velocity between flowing platelets and those at rest on the thrombus exceeded the threshold of U_{act}. However, in case 4, in which all receptors were functional, the aggregate became higher than 12 μm. The vWF-GP Ibα interaction, which is efficient even at high shear, allowed the Fbg-GP IIb/IIIa interaction to be possible at higher positions where high velocity differences can occur. In

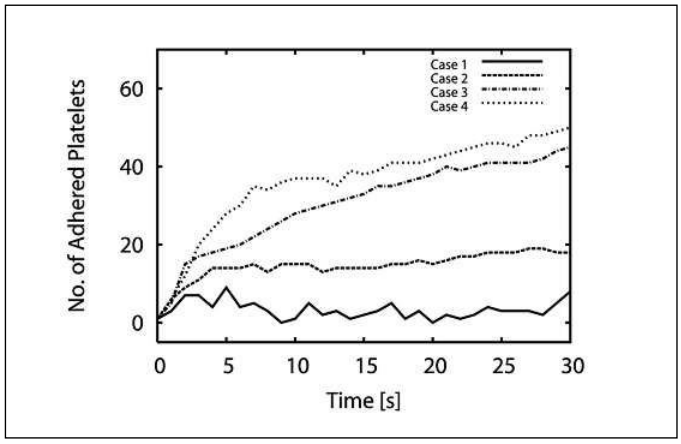

Figure 7: Time course of the number of platelet particles adhered to the blood vessel wall. A significant increase in the number occurred only in cases 3 and 4. The difference in the number of adhered platelet particles was not remarkable between cases 3 and 4, although it was somewhat larger in case 4. In case 2, the number of adhered platelet particles was less than 20 because of transient adhesion.

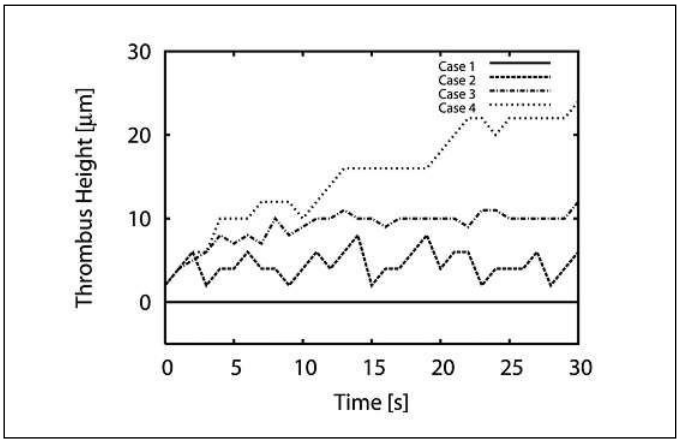

Figure 8: Time course of the maximum thrombus height. Significant platelet aggregation occurred only in cases 3 and 4, in which irreversible platelet adhesion occurred. The height of the thrombus in case 3 did not exceed 12 μm, whereas the thrombus in case 4 was up to 24 μm in height at 30 s.

case 2, the incidental formation of aggregates occurred, but was transient (Fig. 8).

To demonstrate the reliability of our results, we compared them with previous experimental results. Goto et al. (5) examined the effect of the inhibition of GP Ibα and GP IIb/IIIa on the extent of platelet aggregation at a shear rate of 5,400 s^{-1}; thus, the experimental conditions were similar to those in our computations. Goto et al. (5) observed that platelets can aggregate only when both the Fbg-GP IIb/IIIa and vWF-GP Ibα interactions can occur. Our results qualitatively agree with these general observations, indicating that the significant development of thrombus height requires both GP Ibα and GP IIb/IIIa. This agreement of simulation and experimental results qualitatively validates our model, in which some rules for the associations of vWF-GP Ibα and Fbg-GP IIb/IIIa were determined phenomenologically.

Our results suggest that the consideration of the distinct roles of Fbg and vWF is essential in investigating the physiological and pathophysiological mechanisms of thrombus formation using a computational approach. The methods proposed in previous computational analyses (13–19), which did not consider a distinction between these two proteins, cannot reproduce the phenomena that were observed in in-vitro experiments (5); our model does reproduce these phenomena. This implies that our proposed model has the potential to answer questions regarding the pathophysiological mechanisms of thrombus formation such as why a thrombus progresses at sites of disease, e.g. in atherosclerosis, and obstructs the vessel lumen, but does not develop to the point of obstruction in physiological haemostasis.

Our results should be interpreted under the following limitations. First, the simulation was conducted using a monolayer system. Extending the model to a three-dimensional system may quantitatively affect the results. Second, our parameter setting does not consider the precise biochemical behavior of the proteins. Rather, the parameter values for the proteins were set phenomenologically and were static. However, vWF can change in size depending on the magnitude of the shear rate that it experiences (28). Thus, the proteins exhibit highly dynamic behavior under blood flow, which may affect the process of thrombus formation. Dynamic and biochemically reliable parameter settings should be introduced into the model in the future. A possible method for predicting these parameters may be through the use of molecular dynamics. Neglecting vWF-GP IIb/IIIa associations is another limitation in the present study. Considering vWF-GP IIb/IIIa associations might be essential for quantitative observation, and we need to investigate it in further study. However, we expect that vWF-GP IIb/IIIa associations are qualitatively not significant. The previous experiments have shown that functional inhibition of the GP IIb/IIIa does not significantly abolish the interaction of platelets through vWF (4).

Conclusion

We proposed a method based on Stokesian dynamics that simulates thrombus formation under simple shear flow while taking into account the distinct behaviors of two different plasma proteins, vWF and Fbg. We conducted computations for four different situations with respect to deficiencies of the receptors GP Ibα and GP IIb/IIIa, corresponding to previous experimental conditions (5). There was qualitative agreement between the simulation and experimental results. The significant development of thrombus height requires both vWF-GP Ibα and Fbg-GP IIb/IIIa interactions. The consideration of the distinct roles of vWF and Fbg is essential in investigating the physiological and pathophysiological mechanisms of thrombus formation using computational approaches. Although it is necessary to account for the dynamic biochemical behavior of the proteins in future studies, our model may be a powerful tool for answering questions regarding the pathophysiological mechanisms of thrombus formation.

Acknowledgements

This research was supported by "Revolutionary Simulation Software (RSS21)" project supported by next-generation IT program of Ministry of Education, Culture, Sports, Science and Technology (MEXT), Grants in Aid for Scientific Research by the MEXT and JSPS Scientific Research in Priority Areas (768) "Biomechanics at Micro- and Nanoscale Levels", and Scientific Research(A) No.16200031 "Mechanism of the formation, destruction, and movement of thrombi responsible for ischemia of vital organs." Daisuke Mori acknowledges the support of the Tohoku University 21 COE Program, "Future Medical Engineering Based on Bio-nanotechnology."

References

1. Ruggeri ZM. Platelets in atherothrombosis. Nature Med 2002; 8: 1227–1234.
2. Rao AK, Holmsen H. Congenital disorders of platelet function. Semin Hematol 1986; 23: 102–118.
3. Goto S, Salomon DR, Ikeda Y, et al. Characterization of the unique mechanism mediating the shear-dependent binding of soluble von Willebrand factor to platelets. J Biol Chem 1995; 270: 23352–23361.
4. Savage B, Saldivar E, Ruggeri ZM. Initiation of platelet adhesion by arrest onto fibrinogen or translocation on von Willebrand factor. Cell 1996; 84: 289–297.
5. Goto S, Ikeda Y, Saldivar E, et al. Distinct mechanisms of platelet aggregation as a consequence of different shearing flow conditions. J Clin Invest 1998; 101: 479–486.
6. Lefkovits J, Plow EF, Topol EJ. Platelet glycoprotein IIb/IIIa receptors in cardiovascular medicine. New Engl J Med 1995; 332: 1553–1559.
7. Ruggeri ZM. Von Willebrand factor and the mechanisms of platelet functions. Springer-Verlag; 1998.
8. Ruggeri ZM. Platelet interactions with vessel wall components during thrombogenesis. Blood Cells Mol Dis 2006; 36: 145–147.
9. Hennan JK, Swillo RE, Morgan GA, et al. Pharmacologic inhibition of platelet vWF-GPIb alpha interaction prevents coronary artery thrombosis. Thromb Haemost 2006; 95: 469–475.
10. Penz SM, Reininger AJ, Toth O, et al. Glycoprotein Ibalpha inhibition and ADP receptor antagonists, but not aspirin, reduce platelet thrombus formation in flowing blood exposed to atherosclerotic plaques. Thromb Haemost 2007; 97: 435–443.
11. Ruggeri ZM. Von Willebrand factor: looking back and looking forward. Thromb Haemost 2007; 98: 55–62.
12. Wadanoli M, Sako D, Shaw GD, et al. The von Willebrand factor antagonist (GPG-290) prevents coronary thrombosis without prolongation of bleeding time. Thromb Haemost 2007; 98: 397–405.
13. Fogelson AL. Continuum models of platelet-aggregation – Formulation and mechanical-properties. Siam J Appl Math 1992; 52: 1089–1110.
14. Wang NT, Fogelson AL. Computational methods for continuum models of platelet aggregation. J Comp Phys 1999; 151: 649–675.
15. Tamagawa M, Matsuo S. Predictions of thrombus formation using lattice Boltzmann method – (Modeling of adhesion force for particles to wall). Japan Soc Mechan Eng Int J C-Mechanical Systems Machine Elements and Manufacturing 2004; 47: 1027–1034.
16. Kamada H, Tsubota K, Wada S, et al. Computer simulation of formation and collapse of primary thrombus due to platelet aggregation using particle method. Transact Japan Soc Mechan Eng B 2006; 72: 1109–1115.
17. Pivkin IV, Richardson PD, Karniadakis G. Blood flow velocity effects and role of activation delay time on growth and form of platelet thrombi. Proc Natl Acad Sci USA 2006; 103: 17164–17169.
18. Miyazaki H, Yamaguchi T. Formation and destruction of primary thrombi under the influence of blood flow and von Willebrand factor analyzed by a discrete element method. Biorheology 2003; 40: 265–272.
19. Yano K, Mori D, Tsubota K, et al. Analysis of Destruction Process of the Primary Thrombus Under the Influence of the Blood Flow. J Biomech Sci Eng 2007; 2: 34-44**.**
20. Weiss HJ, Rogers J. Fibrinogen and platelets in the primary arrest of bleeding. Studies in two patients with congenital afibrinogenemia. New Engl J Med 1971; 285: 369–374.
21. Tschopp TB, Weiss HJ, Baumgartner HR. Decreased adhesion of platelets to subendothelium in von Willebrand's disease. J Lab Clin Med 1974; 83: 296–300.
22. Ruggeri ZM. von Willebrand factor and fibrinogen. Curr Opin Cell Biol 1993; 5: 898–906.
23. Satoh A, Chantrell RW, Coverdale GN, et al. Stokesian Dynamics Simulations of Ferromagnetic Colloidal Dispersions in a Simple Shear Flow. J Colloid Interface Sci 1998; 203: 233–248.
24. Satoh A. Comparison of approximations between additivity of velocities and additivity of forces for Stokesian dynamics methods. J Colloid Interface Sci 2001; 243: 342–350.
25. Durlofsky L, Brady JF, Bossis G. Dynamic Simulation of Hydrodynamically Interacting Particles. J Fluid Mech 1987; 180: 21–49.
26. Frojmovic MM, Milton JG. Human platelet size, shape, and related functions in health and disease. Physiol Rev 1982; 62: 185–261.
27. Kim S, Karrila SJ. Microhydrodynamics: Principles and Selected Applications. Butterworth-Heinemann, Stoneham; 1991.
28. Siedlecki CA, Lestini BJ, Kottke-Marchant KK, et al. Shear-dependent changes in the three-dimensional structure of human von Willebrand factor. Blood 1996; 88: 2939–2950.